



Cite this: *Dalton Trans.*, 2020, **49**, 6532

Received 3rd March 2020,  
Accepted 20th April 2020

DOI: 10.1039/d0dt00807a

rsc.li/dalton

# Neutral binary chalcogen–nitrogen and ternary S, N,P molecules: new structures, bonding insights and potential applications

Tristram Chivers \*<sup>a</sup> and Risto S. Laitinen \*<sup>b</sup>

Early theoretical and experimental investigations of inorganic sulfur–nitrogen compounds were dominated by (a) assessments of the purported aromatic character of cyclic, binary S,N molecules and ions, (b) the unpredictable reactions of the fascinating cage compound S<sub>4</sub>N<sub>4</sub>, and (c) the unique structure and properties of the conducting polymer (SN)<sub>x</sub>. In the last few years, in addition to unexpected developments in the chemistry of well-known sulfur nitrides, the emphasis of these studies has changed to include nitrogen-rich species formed under high pressures, as well as the selenium analogues of well-known S,N compounds. Novel applications have been established or predicted for many binary S/Se,N molecules, including their use for fingerprint detection, in optoelectronic devices, as high energy-density compounds or as hydrogen-storage materials. The purpose of this perspective is to evaluate critically these new aspects of the chemistry of neutral, binary chalcogen–nitrogen molecules and to suggest experimental approaches to the synthesis of target compounds. Recently identified ternary S,N,P compounds will also be considered in light of their isoelectronic relationship with binary S,N cations.

## 1. Introduction

In contrast to the oxides of nitrogen NO, NO<sub>2</sub>, and N<sub>2</sub>O<sub>x</sub> ( $x = 1, 3, 5$ ), which all have acyclic structures, sulfur and nitrogen form a variety of neutral binary compounds with cyclic, poly-cyclic or polymeric structures.<sup>1</sup> These include the intriguing,

<sup>a</sup>Department of Chemistry, University of Calgary, AB, Canada, T2N 1N4.

E-mail: chivers@ucalgary.ca

<sup>b</sup>Laboratory of Inorganic Chemistry, Environmental and Chemical Engineering, University of Oulu, P. O. Box 3000, 90014, Finland. E-mail: risto.laitinen@oulu.fi



Tristram Chivers

Tristram Chivers, a native of Bath, England, received his BSc, PhD (with Prof. R. D. Chambers FRS) and DSc degrees all from the University of Durham (UK). He joined the University of Calgary in 1969 and served as Head of the Chemistry Department from 1977 to 1982. He is currently Professor Emeritus of Chemistry. His research interests are in the area of main group element chemistry with an emphasis on chalcogen

compounds and inorganic ring systems. He is the author of two books: “A Guide to Chalcogen–Nitrogen Chemistry” and (with I. Manners) “Inorganic Rings and Polymers of the p-Block Elements: From Fundamentals to Applications”.



Risto S. Laitinen

Risto S. Laitinen received his Ph. D. (eng) in 1982 from Helsinki University of Technology (Finland). He joined University of Oulu in 1988 and is currently Professor Emeritus of inorganic chemistry. He has been the Head of Chemistry Department in 1993–2013 and the head of Research Unit of Environmental and Chemical Engineering in 2017–2019. His research activities comprise experimental and computational

main group chemistry, in particular chemistry of chalcogens. He has edited two books: “Selenium and Tellurium Chemistry: From Small Molecules to Biomolecules and Materials” (with J. D. Woollins) and “Selenium and Tellurium Reagents in Chemistry and Materials Science” (with R. Oilunkaniemi).



orange cage molecule  $E_4N_4$  (**1**,  $E = S$ ) with  $D_{2d}$  symmetry,<sup>2a</sup> the colourless, planar four-membered ring  $E_2N_2$  (**2**,  $E = S$ ),<sup>2b</sup> and the blue-black polymer  $(SN)_x$  (**3**),<sup>2c</sup> which becomes superconducting at 0.26 K. Less well-known are the red, six-membered ring  $1,3-S_4N_2$  (**4**),<sup>2d</sup> which adopts a half-chair conformation, and the explosive  $S_5N_6$  (**5**),<sup>2e</sup> an orange compound with a cradle-like structure (Scheme 1). A labile  $-N=S=N-$  bridging unit is a common feature of both **4** and **5**. The extremely hazardous selenium nitride  $Se_4N_4$  (**1**,  $E = Se$ )<sup>3a</sup> has a cage structure similar to that of the sulfur analogue as does the mixed chalcogen nitride  $1,5-Se_2S_2N_4$ .<sup>3b</sup> The binary selenium nitride  $Se_2N_2$  (**2**,  $E = Se$ ) has not been identified as the free ligand, but both main-group metal and transition-metal complexes have been structurally characterised.<sup>3c,d</sup> The six-membered ring  $1,3-Se_4N_2$  (**4**,  $E = Se$ ) is unknown,<sup>4</sup> consistent with *ab initio* molecular orbital calculations for the  $S_xSe_{4-x}N_2$  ring systems. The stability of these ternary chalcogen nitrides is estimated to decrease with increasing selenium content and those that contain an  $-N=Se=N-$  fragment were found to be less stable than those that incorporate an  $-N=S=N-$  moiety.<sup>5</sup>

Early studies of cyclic  $S,N$  species, including cations and anions as well as neutral molecules, focussed on the proposed aromatic character of planar ring systems as well as the properties and possible applications of the conducting polymer  $(SN)_x$ . For example, the following species were considered to be aromatic on the basis of the Hückel  $4n + 2\pi$ -electron rule:  $S_2N_2$  ( $6\pi$ ),  $S_3N_3^-$  ( $10\pi$ ),  $S_4N_3^+$  ( $10\pi$ ) and  $S_5N_5^+$  ( $14\pi$ ).<sup>1a</sup> A fuller understanding of (a) the nature of the transannular  $E\dots E$  interactions in  $E_4N_4$  (**1**,  $E = S, Se$ ) and related bicyclic sulfur-nitrogen molecules,<sup>6,7</sup> (b) the electronic structures of the chalcogen nitrides  $E_2N_2$  (**2**,  $E = S, Se$ ), and (c) the mechanism of the topochemical polymerisation of  $S_2N_2$  rings to generate the polymer  $(SN)_x$  continues to occupy the attention of computational chemists.<sup>8</sup> Furthermore, the serendipitous finding by Kelly and co-workers *ca.* 12 years ago that  $S_2N_2$  vapour interacts with fingerprints on a glass vial to give a visible image of  $(SN)_x$  has now reached the stage of potential commercial applications in forensic science.<sup>9</sup> This development has generated impetus to the search for practical uses of other binary chalcogen-nitrogen species both known and unknown.

In the foregoing context nitrogen-rich chalcogen nitrides have been neglected, undoubtedly as a result of the difficulty in handling these energy-rich systems. However, recent experimental and computational studies of sulfur-nitrogen and selenium-nitrogen species under high pressure have revealed the formation or prediction of a number of novel binary chalcogen

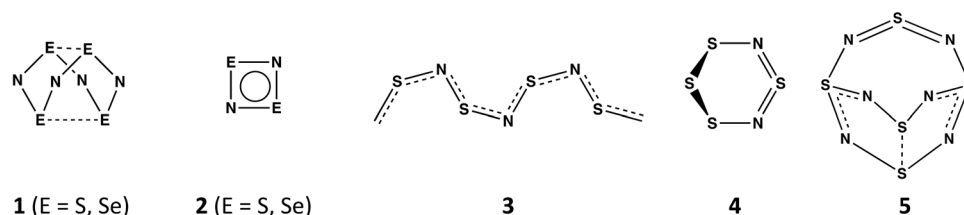
nitrides with unique structures and properties. In a similar vein optoelectronic or mechanical applications have been predicted for the as-yet-unknown sulfur-rich nitride  $S_3N_2$ .<sup>10</sup> The focus of this perspective is an appraisal of recent experimental and computational studies of the structures and properties of both known and new binary chalcogen nitrides with an emphasis on the potential applications of these materials.<sup>11</sup> The chemistry of the less well-studied selenium nitrides will be compared with that of sulfur nitrides throughout the discussion.

The article is organised by considering sulfur-rich nitrides  $S_xN_2$  ( $x = 3, 4$ ) initially, followed by new developments in the chemistry of molecules containing equal numbers of chalcogen and nitrogen atoms as exemplified by compounds **1–3**. The treatise then focusses on the synthesis, unusual structures and predicted properties of nitrogen-rich chalcogen nitrides. Finally, the significance of the recent characterisation of both acyclic and cyclic  $S,N,P$  molecules<sup>12a,b</sup> will be evaluated in the context of the isoelectronic relationship of these ternary species with known binary  $S,N$  cations.<sup>1a,b</sup>

## 2. Sulfur-rich sulfur nitrides $S_3N_2$ and $S_4N_2$

The structures and properties of the sulfur-rich nitrides  $1,3-S_3N_2$  and  $1,3-S_4N_2$  (**4**) provide an interesting comparison. The putative five-membered ring *cyclo*- $1,3-S_3N_2$  is an antiaromatic ( $8\pi$ -electron) system, whereas the known six-membered ring *cyclo*- $1,3-S_4N_2$  is formally a  $10\pi$ -electron molecule, which adopts a half-chair conformation in the solid state.<sup>2d</sup> The optimised geometries for **4**<sup>13</sup> gave values of S–S and S–N bond lengths that are in close agreement with the experimental data.<sup>2d</sup> For example, the calculated S–S bond length is 2.090 Å,<sup>13</sup> *cf.* 2.061 Å from the X-ray structure.<sup>2d</sup> This congruence establishes confidence in the calculated S–S bond length of 2.302 Å for *cyclo*- $1,3-S_3N_2$ .<sup>13</sup> The elongated S–S bond is presumably a result of inherent strain in the five-membered ring, as suggested by the predicted value of the internal bond angle  $<NSS = 94.5^\circ$ , *cf.*  $105.2^\circ$  in the six-membered ring **4**.<sup>2d</sup>

As an alternative to a cyclic structure, in 2018 Chen and co-workers have proposed a stable two-dimensional trisulfur dinitride with three polymorphs comprised solely of  $\sigma$  bonds.<sup>10a</sup> The crystal structure of the most stable form,  $\alpha$ - $S_3N_2$  (space group *Pmn*21), consists of condensed 12-membered ( $S_6N_6$ ) rings (Fig. 1). The  $S_3N_2$  crystal is predicted to be dynamically,



**Scheme 1** Structures of  $E_4N_4$  ( $E = S, Se$ ),  $E_2N_2$  ( $E = S, Se$ ),  $(SN)_x$ ,  $S_4N_2$  and  $S_5N_6$ .





**Fig. 1** The PBE-predicted 2D crystal structure of  $\alpha$ - $S_3N_2$ :  $a = 4.24$ ,  $b = 8.89$  Å;  $d_1 = 1.81$ ,  $d_2 = 1.72$ ,  $d_3 = 1.66$  Å;  $\theta_1 = 116.8^\circ$ ,  $\theta_2 = 119.3^\circ$ ,  $\theta_3 = 119.2^\circ$ ,  $\theta_4 = 106.1^\circ$ ,  $\theta_5 = 103.7^\circ$ .<sup>10a</sup> Bonding is depicted by an isosurface of the electron density.<sup>10a</sup> (Reproduced with permission from H. Xiao, X. Shi, X. Liao, Y. Zhang and X. Chen, *Phys. Rev. Mater.*, 2018, 2, 024002. © 2018 American Physical Society.)

thermally and chemically stable on the basis of the computed phonon spectrum and *ab initio* molecular dynamics simulations. The predicted “chemical stability” is surprising in view of the known susceptibility of sulfur–nitrogen compounds to degradation by both nucleophiles and electrophiles.<sup>1a,b</sup> Calculations also indicate that  $\alpha$ - $S_3N_2$  will be a wide, direct band gap (3.92 eV) semiconductor with possible optoelectronic applications such as blue or UV light-emitting diodes and photodetectors.

A subsequent study of 2D monolayer crystals of  $E_3N_2$  ( $E = S, Se$ ) employing DFT calculations predicted  $\alpha$ -heart and  $\beta$ -heart structures, which exhibit different mechanical and electrical properties.<sup>10b</sup> The former structure resembles that depicted for  $\alpha$ - $S_3N_2$  in Fig. 1. The  $E_3N_2$  materials are predicted to have unusual mechanical properties as indicated by the values of Negative Poisson’s Ratios indicating auxetic behaviour.<sup>10c</sup>

The recent computational predictions of the unique structure and mechanical properties of  $S_3N_2$  provide a strong incentive for pursuing experimental approaches to this unknown binary sulfur nitride. A carefully controlled cyclocondensation reaction of ClSSCl with  $Me_3SiNSNSiMe_3$  under high-dilution conditions is a plausible first attempt.<sup>14</sup> An alternative route is the one-electron chemical or electrochemical reduction of the known radical cation  $[S_3N_2]^+$ , which is prepared by oxidation of  $S_4N_4$  with  $AsF_5$  in liquid  $SO_2$ .<sup>1a</sup> The reaction of 1,3- $S_4N_2$  (4) with one equivalent of  $PPh_3$  is likely to result in attack of the nucleophile at the S(IV) centre rather than the required removal of a single sulfur atom from the  $-S-S-S-$  unit.

### 3. Molecules with equal numbers of chalcogen and nitrogen atoms

#### 3.1. Tetrasulfur and tetraselenium tetranitride $E_4N_4$ ( $E = S, Se$ )

The  $S_4N_4$  ( $E = S$ ) molecule is regarded as the quintessential binary sulfur–nitrogen compound in view of its multifarious

applications as a reagent in inorganic and organic chemistry, despite a tendency to detonate under the influence of heat or friction.<sup>1a</sup> Notwithstanding the availability of simple synthetic procedures, the selenium analogue **1** ( $E = Se$ ) has undergone limited use for the preparation of selenium–nitrogen compounds owing to the explosive nature of this reagent.<sup>1a,b</sup> Some new aspects of the chemical reactivity of **1** ( $E = S$ ), including the electrochemical reduction and photochemical behaviour, are discussed in a recent book chapter.<sup>1b</sup> This section will consider more recent developments in the chemistry of  $S_4N_4$ , especially those involving an understanding of the electronic structure and unusual reaction chemistry of this cage compound.

**3.1.1. Electronic structure of **1** ( $E = S, Se$ ); transannular  $E \cdots E$  interactions.** The strength of the intramolecular  $S \cdots S$  interaction in **1** ( $E = S$ ) has been estimated to be of the order of a hydrogen bond on the basis of the noncovalent interaction index.<sup>15</sup> Tuononen *et al.*, have investigated the nature of this interaction in **1** ( $E = S, Se$ ) with high-level theoretical methods.<sup>6</sup> Their results showed that the elongation of the transannular  $E \cdots E$  bonds compared to a typical single-bond value can be attributed to surprisingly large correlation effects. Furthermore, there is some singlet diradical character associated with each  $E \cdots E$  interaction. Although the consequences of this feature of the electronic structure of **1** ( $E = S$ ) have not been investigated intentionally by experimentalists, an early report by Mews described the preparation of the di-substituted derivative  $S,S'$ -1,5- $S_4N_4[ON(CF_3)_2]_2$  upon reaction of  $S_4N_4$  with two equivalents of the nitroxide radical  $(CF_3)_2NO^\bullet$ .<sup>16</sup> The reaction of  $S_4N_4$  with molecular  $H_2$  is worthy of investigation computationally and experimentally in view of this diradical character and the potential use of sulfur–nitrogen compounds as hydrogen-storage materials as discussed in section 3.2.5.

A different aspect of the bonding interactions in **1** ( $E = S$ ) was reported in 2016 by Jenkins and co-workers.<sup>17</sup> By applying QTAIM (quantum theory of atoms in molecules) methodology to all 18 modes of vibration of the cage molecule, these authors found a considerable degree of metallicity in the  $S-S$  and  $S-N$  bonding interactions, on the basis of the delocalisation of the electron density away from the atoms. In particular, considerable metallic behaviour was apparent in the  $S-S$  bond critical points for all modes.<sup>17</sup> The experimental implications of this finding are yet to be investigated.

**3.1.2. Unusual reaction chemistry involving  $S_4N_4$ .** Numerous complexes of  $S_4N_4$  with Lewis acids have been structurally characterised and the bonding trends in these N-bonded adducts have been investigated.<sup>1b,18</sup> In 2018 Si and Ganguly described first principles calculations of the interaction of  $S_4N_4$  with benzene and naphthalene.<sup>19</sup> These authors found that the  $\sigma$  hole of the sulfur atoms of  $S_4N_4$  engages in non-covalent interactions with these aromatic  $\pi$ -systems. For example, the interaction energy of  $S_4N_4$  with three naphthalene rings was estimated to be *ca.* 20 kcal mol<sup>−1</sup>.<sup>19</sup> The  $S \cdots \pi$  interaction is the main driving force in these complexes of  $S_4N_4$  with only a marginal contribution from the N atoms. The reactions of  $S_4N_4$  with alkynes have been investigated in con-



siderable details and shown to cause cleavage of the cage molecule to form the heterocycle 1,2,5-thiadiazole as the major product along with the 7-membered rings  $(RC)_2S_3N_3$  and  $RCS_3N_3$ .<sup>1a</sup> The only example of adduct formation between  $S_4N_4$  and an organic compound was reported more than 20 years ago by Konarev *et al.*<sup>20</sup> These authors determined the single crystal X-ray structural analysis of the non-stoichiometric complex  $C_{60}(S_4N_4)_{1.33}(C_6H_6)_{0.67}$  and found that only the sulfur atoms participate in bonding to the fullerene.<sup>20</sup> A more detailed experimental investigation of complexes of  $S_4N_4$  with aromatic systems is warranted in view of the computational predictions.<sup>19</sup>

A convenient synthesis of  $S_4N_4$  involves the cyclocondensation reaction of  $[(Me_3Si)_2N]_2S$  with an equimolar mixture of  $SCl_2$  and  $SO_2Cl_2$ .<sup>21</sup> The complexity of the reaction pathway for this transformation is highlighted on the cover page of a recent textbook with a focus on “arrow-pushing” in inorganic chemistry.<sup>22</sup> Ghosh and Berg propose a twelve-step process with the *sequential* participation of the reagents  $SCl_2$  followed by  $SO_2Cl_2$ . However, the combination of  $SCl_2$  and  $SO_2Cl_2$  generates  $SCl_4$  ( $+SO_2$ ) spontaneously, so a cyclocondensation pathway involving this *in situ* reagent is more likely. The formation of an acyclic  $-SNSNS-$  intermediate and, subsequently, an eight-membered  $S_4N_4$  ring *via* a series of thermodynamically favoured eliminations of  $Me_3SiCl$  is suggested (Scheme 2).

Kumar and Muralidharan have reported the hexamethyldisilazane (HMDS)-assisted synthesis of  $\beta$ - $In_2S_3$ ,  $CuS$  and  $Ag_2S$  nanoparticles *via* reactions of sulfur with an appropriate metal salt in the presence of HMDS.<sup>23</sup> In order to explain the role of HMDS in the synthesis of these metal sulfides, the formation of a novel polymeric intermediate  $[SN(SiMe_3)]_n$  was invoked.<sup>23c,d</sup> The characterization of this purported polymer was based upon GPC (gel permeation chromatography) analysis of the distilled material, as well as  $^{29}Si$  NMR spectra and HRMS (high resolution mass spectrometry) data.<sup>23a</sup> The fact that this intermediate could not be isolated as a pure com-

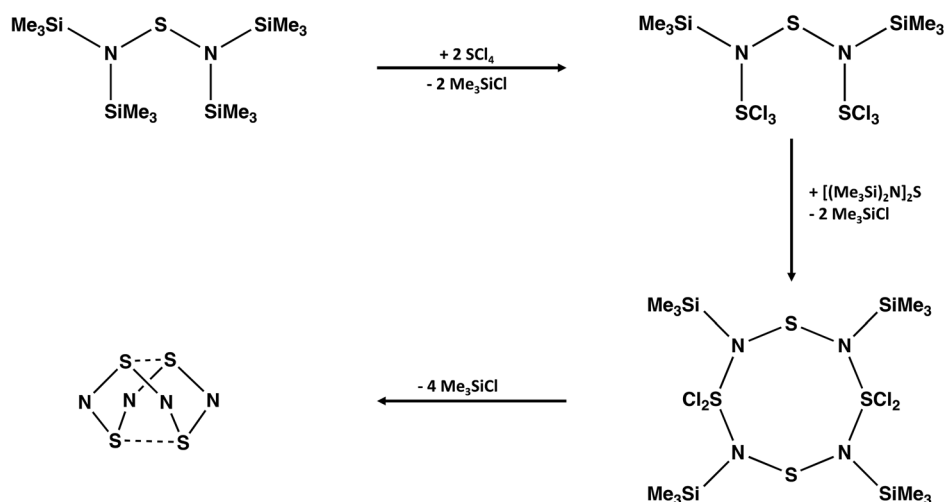
pound was attributed by the authors to the similarity of its boiling point with that of HMDS. Since the boiling point of HMDS is only 125 °C, this explanation is highly unlikely. Orange crystals obtained as a minor by-product in the synthesis of  $Ag_2S$  were identified by XRD as  $S_4N_4$  as a minor by-product;<sup>23b</sup> however, the formation of this binary sulfur nitride from the purported sulfur imide polymer is not readily explained.

### 3.2. Disulfur and diselenium dinitride $E_2N_2$ (2, E = S, Se)

In contrast to the numerous applications of  $S_4N_4$  as a source of novel inorganic and organic sulfur–nitrogen compounds,<sup>1a,b</sup> the use of  $S_2N_2$  in synthesis is rare owing to its highly labile nature. However, both electrochemical and chemical reduction produce the  $[S_3N_3]^-$  anion, which can be isolated as ion-separated salts.<sup>1b,24</sup> This section will consider recent developments in our understanding of the chemistry of  $S_2N_2$  and its heavier chalcogen homologues, including electronic structures, spectroscopic characterisation, the isomers formed upon photolysis, topochemical polymerization to give  $(SN)_x$ , and possible use as a hydrogen-storage material.

**3.2.1. Electronic structures.** The square-planar structure of  $S_2N_2$  (2, E = S), a volatile white crystalline solid, was established 45 years ago.<sup>1a</sup> Despite this longevity, the electronic structure of this four-membered ring and its heavier chalcogen analogues continues to generate controversy centred around their aromaticity and diradical character.<sup>25</sup> The most recent developments are discussed below.

In 2004 Head-Gordon *et al.* concluded that the diradical character of  $S_2N_2$  is not significant on the basis of a large HOMO–LUMO gap (5.1 eV), a large singlet–triplet vertical transition energy (3.6 eV), and the lack of a spin-unrestricted solution at the level of DFT using the B3LYP functional.<sup>26</sup> They asserted, however, that  $S_2N_2$  is aromatic based on its negative NICS value (−26.2 ppm), albeit with a small aromatic stabilisation energy, since only two of the six  $\pi$  electrons contribute to the bonding.



**Scheme 2** Formation of  $S_4N_4$  *via* cyclocondensation of  $[(Me_3Si)_2N]_2S$  with  $SCl_4$ .





Concurrently, Tuononen and co-workers investigated the electronic structures and molecular properties of  $S_2N_2$ ,<sup>27a</sup> as well as the unknown heavier chalcogen analogues  $Se_2N_2$ ,  $SSeN_2$  and  $Te_2N_2$ ,<sup>27b</sup> by employing various computational methods. These authors agreed that all of these four-membered rings can be described as  $2\pi$ -electron aromatics, but with minor singlet diradical character ranging from 6% in  $S_2N_2$  to 10%  $Te_2N_2$  located solely on the two nitrogen atoms.<sup>27b</sup>

In 2012 Braidia *et al.* carried out an *ab initio* valence bond study of  $E_2N_2$  which confirmed that the diradical sites are the two nitrogen atoms ( $E = Se, Te$ ), however they estimated that the contribution from diradical structures is close to 50%.<sup>28</sup> Their calculations of vertical resonance energies gave values of about 80% of the predicted value of benzene for  $S_2N_2$  with somewhat lower values for  $Se_2N_2$  and  $Te_2N_2$ , consistent with the notion of aromatic character for  $S_2N_2$  based on magnetic criteria. An important conclusion from these results is that diradical character and aromaticity are not mutually exclusive.<sup>28</sup> In a sequel to his earlier work on valence bond structures for  $S_2N_2$ , Harcourt<sup>29</sup> postulated that the six Lewis structures assumed by Braidia *et al.*<sup>28</sup> are equivalent to resonance between two *increased-valence* structures with one-electron and fractional electron-pair  $\pi$  bonds.

In 2018 Karadakov *et al.* employed magnetic criteria to study the bonding and aromaticity in the ground, first singlet excited and lowest triplet electronic states of  $S_2N_2$ .<sup>25</sup> Their results indicate that (a) the  $S_0$  electronic state is aromatic, but less so than the electronic ground state of benzene, (b)  $S_1$  is strongly antiaromatic, and (c)  $T_1$  is moderately antiaromatic to a similar extent to that observed in the electronic ground state of square cyclobutadiene. Thus, they assert that  $S_2N_2$  is the first example of an inorganic ring for which theory predicts substantial changes in aromaticity upon vertical transition from the ground state to the first singlet or lowest triplet electronic states.<sup>25</sup>

**3.2.2. Spectroscopic characterisation.** Tuononen *et al.*,<sup>27b</sup> found that coupled cluster and multiconfigurational

approaches, as well as density functional methods, were the most reliable for the prediction of spectroscopic properties such as vibrational frequencies,  $^{14}N$ ,  $^{15}N$  and  $^{77}Se$  NMR chemical shifts, and excitation energies of sulfur and selenium nitrides. The congruence between the computational results and experimental data for  $S_2N_2$  provides some confidence in the predictions for selenium-containing analogues  $SSeN_2$  and  $Se_2N_2$ .

The calculated IR-active vibrational frequencies<sup>27b</sup> are in reasonable agreement with experimental data from the IR and Raman spectra of  $S_2N_2$  obtained as a solid condensate and in  $N_2$  or  $CH_4$  matrices at 15–35 K, which were reported by Downs *et al.*<sup>30</sup> By using 30%  $^{15}N$ -enrichment, these authors confirmed that the isolated  $S_2N_2$  molecule has essentially the same square-planar geometry as the crystalline solid; calculations of the S–N stretching force constant indicated a bond order only slightly greater than 1.<sup>30</sup> In 2014 the high-resolution gas-phase FTIR spectrum of  $S_2N_2$  together with a re-investigation of the IR spectrum in solid argon at 16 K were reported by Perrin, Beckers and co-workers.<sup>31</sup> The main difference between the gas-phase and solid-state structures of  $S_2N_2$  involves the bond angles; in the gas phase the angle at nitrogen  $\angle SNS$  is smaller than  $\angle NSN$ , whereas the opposite is true in the solid-state structures.<sup>31</sup> These small disparities may be the consequence of the intermolecular interactions that occur between  $S_2N_2$  rings in the plane of the chain of rings in the solid state. Cremer *et al.* have computed a pseudorotation barrier of  $<2$  kJ mol<sup>−1</sup> for  $S_2N_2$  indicative of a floppy molecule, however these authors maintain that this characteristic does not alter the electronic structure of the four-membered ring.<sup>32</sup>

The predicted IR and Raman spectra of the selenium-containing systems  $Se_2N_2$  and  $SSeN_2$  are depicted in Fig. 2.<sup>27b</sup> The band at  $\sim 590$  cm<sup>−1</sup> in the IR spectrum of  $Se_2N_2$  should be considerably less intense than the other two bands. In a similar vein, the intensity of the band at 822 cm<sup>−1</sup> is estimated to be more than twice those of the other two bands.

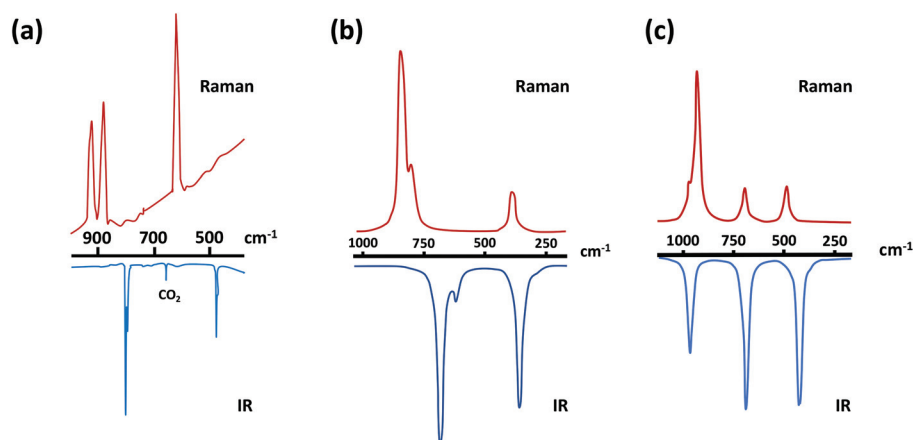


Fig. 2 (a) IR/Raman spectra of  $S_2N_2$ .<sup>30</sup> (Adapted with permission from R. Evans, A. J. Downs, R. Köppe and S. C. Peake, *J. Phys. Chem. A*, 2011, **115**, 5127–5137. © 2011 American Chemical Society), and the theoretically predicted IR/Raman spectra of (b)  $Se_2N_2$  and (c)  $SeSN_2$ .<sup>27b</sup> (adapted with permission from H. M. Tuononen, R. Suontamo, J. Valkonen and R. S. Laitinen, *J. Phys. Chem. A*, 2005, **109**, 6309–6317. © 2005 American Chemical Society).



Tuononen *et al.*, have also calculated the  $^{14}\text{N}$ ,  $^{15}\text{N}$  and  $^{77}\text{Se}$  NMR chemical shifts for the chalcogen nitrides  $\text{S}_2\text{N}_2$ ,  $\text{SeSN}_2$ ,  $\text{Se}_2\text{N}_2$ ,  $\text{S}_4\text{N}_4$  and  $\text{Se}_2\text{S}_2\text{N}_4$ .<sup>27b</sup> Surprisingly, no experimental NMR data are available for  $\text{S}_2\text{N}_2$ . However, the calculated  $^{14}\text{N}$  and  $^{15}\text{N}$  NMR chemical shifts for  $\text{S}_4\text{N}_4$  and the known mixed selenium–sulfur nitride  $\text{Se}_2\text{S}_2\text{N}_4$  are in excellent agreement with the experimental data<sup>3c</sup> providing some confidence in the predicted values of  $95 \pm 20$ ,  $125 \pm 20$  and  $185 \pm 20$  ppm for  $\text{S}_2\text{N}_2$ ,  $\text{SeSN}_2$  and  $\text{Se}_2\text{N}_2$ , respectively. The calculated  $^{77}\text{Se}$  chemical shifts for 1,5- $\text{Se}_2\text{S}_2\text{N}_4$  at different levels of theory are *ca.* 200 ppm lower than experimental values.<sup>3c,27b</sup> By contrast, the calculated PBEPE and CAS  $^{77}\text{Se}$  chemical shifts of 1906 and 1886 ppm for  $\text{Se}_4^{2+}$  are only slightly lower than the experimental value of 1936 ppm. Assuming a similar error for  $\text{SeSN}_2$  and  $\text{Se}_2\text{N}_2$ ,  $^{77}\text{Se}$  chemical shifts of  $1820 \pm 20$  and  $1780 \pm 20$  ppm, respectively, are estimated for these structurally analogous four-membered rings.<sup>27b</sup> The ternary chalcogen nitride  $\text{SeSN}_2$  has been proposed as an intermediate in the formation of 1,5- $\text{Se}_2\text{S}_2\text{N}_4$  from reactions of  $(\text{Me}_3\text{SiNSN})_2\text{E}$  ( $\text{E} = \text{S}, \text{Se}$ ) with  $\text{E}'\text{Cl}_2$  ( $\text{E}' = \text{S}, \text{Se}$ ),<sup>3c</sup> but this potential precursor of a mixed sulfur–selenium nitride polymer  $(\text{SNSN})_x$  has eluded isolation.

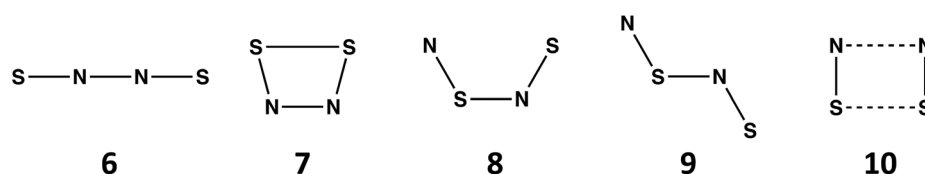
The experimental UV spectrum of  $\text{S}_2\text{N}_2$  consists of a broad band in the range 4.5–5.8 eV comprised of two overlapping absorptions centred at approximately 5.0 eV ( $\sim 250$  nm) which is attributed to the  $\pi \rightarrow \pi^*$  electronic transition.<sup>33</sup> The calculated band-gap energies decrease as the selenium content in the ring increases as illustrated by colourless  $\text{S}_2\text{N}_2$  (3.32 eV,  $\sim 375$  nm) the predicted orange-yellow colour of  $\text{SSeN}_2$  (2.50 eV,  $\sim 495$  nm) and red colour of  $\text{Se}_2\text{N}_2$  (2.20 eV,  $\sim 560$  nm).<sup>27b</sup> This information should be valuable for the identification of the selenium-containing four-membered rings.

**3.2.3. Photolysis: isomers of  $\text{S}_2\text{N}_2$ .** In 2015 Zeng, Beckers and co-workers investigated the UV photolysis of  $\text{S}_2\text{N}_2$  in solid argon matrices using two different light sources ( $\lambda = 248$  or 255 nm).<sup>34</sup> Although calculations predict both linear SNNS (6) and cyclic 1,2,3,4-dithiadiazete ( $\text{C}_{2v}$ ) (7) to be lower in energy than the familiar cyclic  $\text{S}_2\text{N}_2$  ( $\text{D}_{2h}$ ) (2,  $\text{E} = \text{S}$ ),<sup>14</sup> neither of these two isomers has been observed experimentally. Instead, by employing IR spectra of both natural abundance and  $^{15}\text{N}$ -enriched  $\text{S}_2\text{N}_2$ , these authors were able to identify two open shell isomers, *trans*-SNSN (8) and *cis*-SNSN (9), as well as a closed shell  $\text{C}_{2v}$  dimer  $(\text{SN})_2$  (10), as the primary photolysis products (Scheme 3).<sup>34</sup> The identification of the open shell isomers is relevant to the mechanism of polymerisation of  $\text{S}_2\text{N}_2$  into  $(\text{SN})_x$ , which is discussed in the next section.

**3.2.4. Topochemical polymerisation to  $(\text{SN})_x$ : applications in forensic science.** The spontaneous topochemical polymerisation of  $\text{S}_2\text{N}_2$  into  $(\text{SN})_x$ , a polymer with fascinating conducting properties, has been known for more than 40 years.<sup>2c</sup> Kelly *et al.*, have demonstrated that this process can be achieved in the zeolite Na-ZSM-5, which has a pore size that is able to accommodate  $\text{S}_2\text{N}_2$  as well as infinite channels along the *b*-axis to allow for polymer growth.<sup>9a</sup> The same group also reported that the exposure of fingerprints on various surfaces, *e.g.* glass, metal, paper or ceramic surfaces, to  $\text{S}_2\text{N}_2$  vapour generated an image of the fingerprint due to the formation of blue-black  $(\text{SN})_x$  polymer (Fig. 3a).<sup>9b,c</sup> It was suggested that this serendipitous observation could have applications in forensic science, although the design of a practical and portable apparatus for the production of  $\text{S}_2\text{N}_2$  was recognised as a major impediment. However, in 2019 a collaborative effort with industrial and government laboratories described a comparison of the  $\text{S}_2\text{N}_2$  process with other methods for fingerprint detection and found it to be effective with the potential for improvements over existing processes. Crucially, this study relied on a safe-to-handle, but unidentified, precursor that is rapidly decomposed to  $\text{S}_2\text{N}_2$ . The experimental set-up is illustrated in Fig. 3b.<sup>9d</sup>

In 2013 Takaluoma *et al.* carried out molecular dynamics simulations of the topochemical polymerisation of  $\text{S}_2\text{N}_2$  in the solid state using DFT methods and periodic functions.<sup>8</sup> The calculations involved both high pressures and slightly elevated temperatures in order to increase the reaction rate. The formation of  $(\text{SN})_x$  is initiated by cleavage of one S–N bond in  $\text{S}_2\text{N}_2$  followed by a very rapid attack of the resulting open-chain isomer, *e.g.* 8 in Scheme 3, on a neighbouring ring (Fig. 4). Propagation occurs along the *a* axis throughout the lattice. The packing changes from the herringbone structure of the  $\text{S}_2\text{N}_2$  lattice to the layered structure of  $(\text{SN})_x$ . Although the metrical data for the polymer chain are in good agreement with the experimental crystal structure, there is less long-range order between neighbouring chains, possibly due to the influence of pressure or the poor description of dispersion by density functional theory.<sup>8</sup>

**3.2.5. A hydrogen-storage material?** Datta has described quantum chemical investigations of the interaction of  $\text{H}_2$  molecules with binary S,N rings including  $\text{S}_2\text{N}_2$ .<sup>35</sup> An adduct of  $\text{S}_2\text{N}_2$  with two molecules of  $\text{H}_2$  located in an eclipsed fashion above and below the ring was found to have only dispersive interactions with a low binding energy ( $< -1.5$  kcal mol<sup>-1</sup>). However, when the ring is doped with a transition metal such as Ni(0), Pd(0) or Pt(0), complexes that incorporate



**Scheme 3** Structural arrangements of planar cyclic and acyclic isomers of  $\text{S}_2\text{N}_2$ .<sup>34</sup>



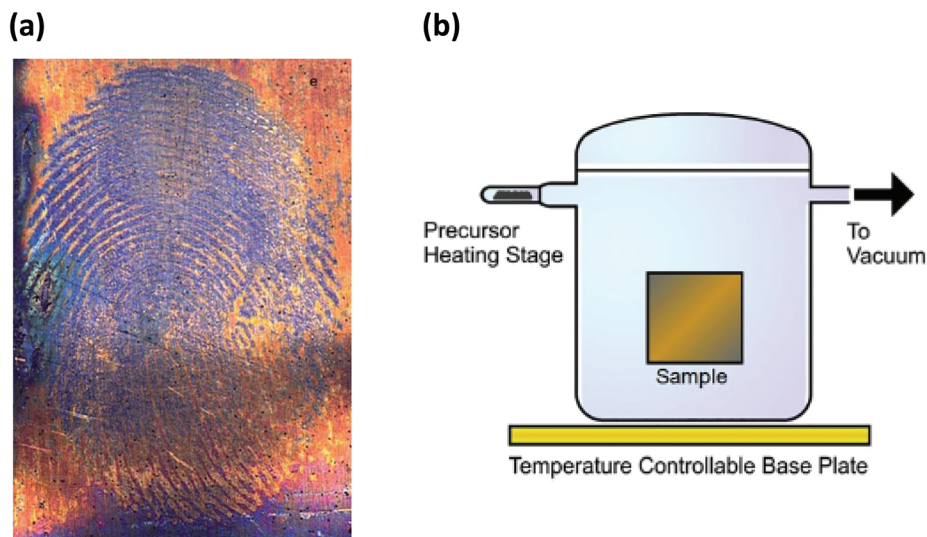


Fig. 3 (a) Formation of (SN)<sub>x</sub> over latent fingerprints on metallic surfaces<sup>9c</sup> (reproduced with permission from S. M. Bleay, P. F. Kelly, R. S. B. King, *J. Mater. Chem.*, 2010, 20, 10100–10102. © 2010 The Royal Society of Chemistry.). (b) Diagram of S<sub>2</sub>N<sub>2</sub> processing equipment<sup>9d</sup> (reprinted with permission from S. M. Bleay, P. F. Kelly, R. S. P. King and S. G. Thorngate, *Sci. Justice*, 2019, 59, 606–621. © 2019 Elsevier B. V.).

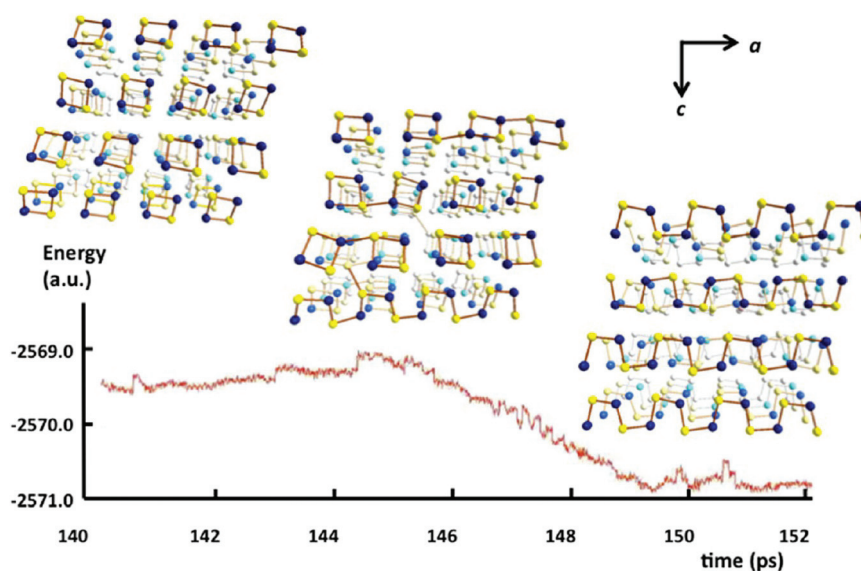


Fig. 4 Simulated energy profile of the topochemical polymerisation of S<sub>2</sub>N<sub>2</sub> rings to (SN)<sub>x</sub> at 50 GPa and 600 K. Sulfur atoms are indicated by yellow spheres and nitrogen atoms by blue spheres (*b* axis is directed away from the reader).<sup>8</sup> (Reproduced with permission from T. T. Takaluoma, K. Laasonen and R. S. Laitinen, *Inorg. Chem.*, 2013, 52, 4648–4657. © 2013 American Chemical Society.)

three H<sub>2</sub> molecules for each metal centre were found to have binding energies of −67.75, −18.73 and −81.75 kcal mol<sup>−1</sup> for M = Ni, Pd and Pt, respectively. As illustrated in Fig. 5, the binding modes of H<sub>2</sub> to the metal centre are markedly different. In the Ni and Pd complexes four H atoms appear as hydrides while one H<sub>2</sub> molecule is η<sup>2</sup>-coordinated to the metal. By contrast, in the most stable Pt complex all six hydrogen atoms exist as hydrides with five of them forming an almost regular pentagon.<sup>35</sup> Although the practicality of using binary S, N compounds as hydrogen-storage materials may be ques-

tioned by experimentalists, investigations of the interaction of extended systems similar to (SN)<sub>x</sub> may be worthy of experimental interrogation.

## 4. Nitrogen-rich chalcogen nitrides

Early work on nitrogen-rich sulfur nitrides such as SN<sub>2</sub> and SN<sub>4</sub> was mainly limited to the purported involvement of these species as fleeting intermediates. However, recent experi-



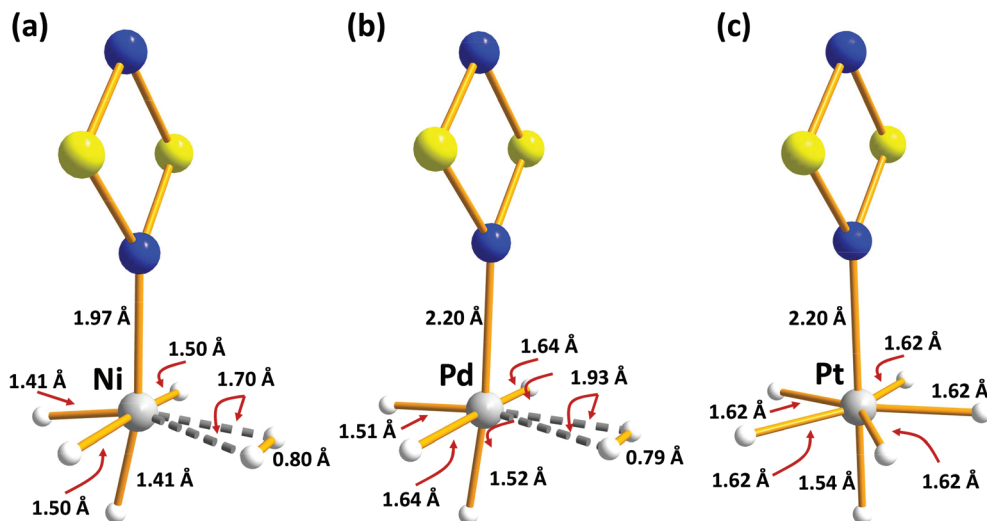


Fig. 5 B3LYP/6-31G(d,p) optimised structures of  $\text{H}_2$ -absorbed metal-doped  $\text{S}_2\text{N}_2$  (a)  $\text{M} = \text{Ni}$  (b)  $\text{M} = \text{Pd}$  (c)  $\text{M} = \text{Pt}$  (redrawn from computational data in ref. 35).

mental and theoretical investigations of the formation and structures of this class of sulfur nitrides and their selenium analogues under high pressure have revealed fascinating properties with potential applications in optoelectronics and as high-energy-density materials. This section is organised according to increasing nitrogen content of these binary molecular species. Nitrogen-rich selenium nitrides are discussed in section 4.4.

#### 4.1. The isomers NNS and NSN

The lowest energy isomer NNS, a heavier analogue of the stable molecule  $\text{N}_2\text{O}$ , decomposes above 160 K. It is generated by flash photolysis of 5-phenyl-1,2,3,4-thiadiazole and has been characterised by high-resolution mass spectrometry and IR spectroscopy.<sup>36</sup> The symmetrical isomer NSN has been invoked as an elimination product during the transformations

of polycyclic S-N compounds,<sup>1a</sup> but the synthesis and structure of this simple sulfur nitride remained elusive until very recently (*vide infra*).

In 2016 Zhang and co-workers investigated the stability, electronic structure and optical properties of a  $P3m1$  phase of  $1T\text{-EN}_2$  ( $\text{E} = \text{S}, \text{Se}, \text{Te}$ ) by means of DFT calculations (the prefix  $1T$  refers to one layer per trigonal unit cell).<sup>37</sup> The calculated crystal structure of the two-dimensional material  $1T\text{-SN}_2$  is comprised of six-coordinated S atoms and three-coordinate N centres (Fig. 6a). These chalcogen nitrides  $1T\text{-EN}_2$  ( $\text{E} = \text{S}, \text{Se}, \text{Te}$ ) are endothermic materials.  $1T\text{-SN}_2$  has dynamical stability based on phonon spectra and calculated cohesive energies, but the thermal and mechanical stabilities have yet to be determined. Band-structure calculations revealed indirect band gaps of 2.825, 2.351, and 2.336 eV for  $1T\text{-SN}_2$ ,  $1T\text{-SeN}_2$ , and  $1T\text{-TeN}_2$ , respectively. Furthermore, the application of biaxial

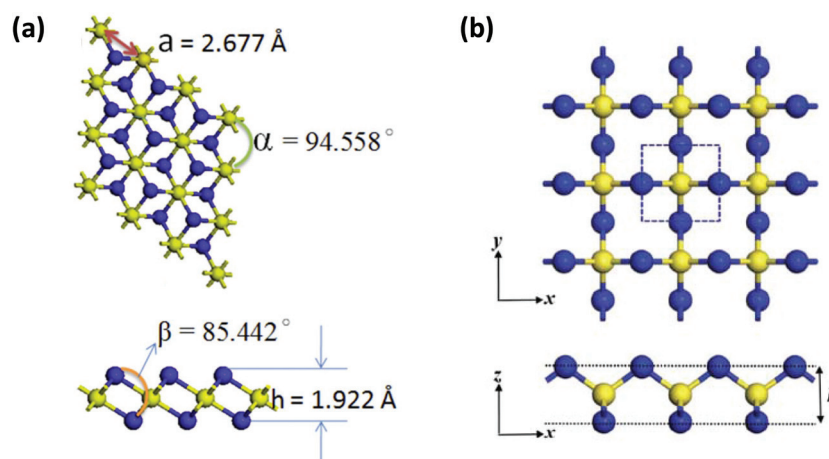


Fig. 6 Optimised structures of (a)  $1T\text{-SN}_2$ <sup>37</sup> (reproduced with permission from J.-H. Lin, H. Zhang, X.-L. Cheng and Y. Miyamoto, *Phys. Rev. B*, 2016, **94**, 195404. © 2016 American Physical Society), and (b)  $\text{S-SN}_2$ <sup>38</sup> (reproduced with permission from F. Li, X. Lv, J. Gu, K. Tu, J. Gong, P. Jin and Z. Chen, *Nanoscale*, 2020, **12**, 85–92. © 2020 The Royal Society of Chemistry).





strain induced a transition from a wide-band-gap semiconductor to a metal. These findings suggest that the binary chalcogen nitrides  $1T\text{-EN}_2$  are promising materials for applications in optoelectronic devices.<sup>37</sup>

Earlier this year Chen and co-workers proposed a new phase of the  $\text{SN}_2$  monolayer, namely  $S\text{-SN}_2$ , by using first-principles calculations combined with the particle-swarm optimisation method.<sup>38</sup> The structure of  $S\text{-SN}_2$  belongs to the space group  $P4M2$  and incorporates four-coordinate S atoms and two-coordinate nitrogen centres (Fig. 6b); the prefix  $S$  is used to indicate its square lattice and, hence, distinguish this new structure from  $1T\text{-SN}_2$ . The  $S\text{-SN}_2$  monolayer is a remarkably stable semi-conductor with an indirect band gap of 2.79 eV, *cf.* 2.825 eV for  $1T\text{-SN}_2$ .<sup>37</sup> The co-existence of both out-of-plane and in-plane negative Poisson's ratios indicates 3D auxetic properties for this new material,<sup>10c</sup> which may have applications in mechanical or optoelectronics devices.

In 2017 Cui and co-workers performed particle-swarm optimisation calculations on the sulfur-nitrogen system up to 200 GPa.<sup>39</sup> Three binary sulfur-nitrogen solids were determined to be thermodynamically stable:  $Pnma$  ( $\text{SN}$ )<sub>x</sub>,  $Pnnm$   $\text{SN}_2$ , and  $C2/c$   $\text{SN}_4$  at pressures of 37, 43 and 48 GPa, respectively. Their crystal structures are depicted in Fig. 7. A polymeric 3D arrangement was predicted for  $\text{SN}_2$  (Fig. 8c). Partial density of states calculations indicated that  $\text{SN}_2$  is a semiconductor with a direct band gap of 0.66 eV at 60 GPa.

Last year a seminal experimental investigation of the formation of sulfur nitrides in the  $\text{S-N}_2$  system at high pressures by Laniel and co-workers confirmed the predictions for  $\text{SN}_2$ . These authors found that the reaction of elemental sulfur and  $\text{N}_2$  gas in a diamond anvil cell at pressures above 60 GPa with laser heating produces an orthorhombic ( $Pnnm$ )  $\text{SN}_2$  compound.<sup>40</sup> The lattice parameters of this material obtained from powder diffraction data match closely the theoretically pre-

dicted crystalline structure of  $\text{SN}_2$ .<sup>37</sup> Single crystal X-ray diffraction analysis revealed a  $\text{CaCl}_2$ -type structure composed of edge-sharing  $\text{SN}_6$  octahedra with N atoms that are triply coordinated by S atoms (Fig. 8).<sup>40</sup> The  $\text{SN}_2$  solid was found to be metastable down to *ca.* 20 GPa, at which point it dissociates into its elements.<sup>40</sup>

#### 4.2. Thiatetrazole $\text{SN}_4$

The nitrogen-rich thiatetrazole  $\text{SN}_4$  has attracted the attention of both experimental and theoretical chemists for more than 20 years. Klapötke and Schulz attempted to prepare  $\text{SN}_4$  from the reaction of the cation  $[\text{NS}]^+$  in  $[\text{NS}][\text{AsF}_6]$  with the azide ion  $[\text{N}_3]^-$  in cesium azide. The final product was a black precipitate identified as the polymer  $(\text{SN})_x$ ; no experimental evidence ( $^{14}\text{N}$  NMR) could be found for the expected  $\text{SN}_4$  intermediate.<sup>41</sup> Furthermore, no spectroscopic evidence for the formation of  $\text{SN}_4$  was garnered from the recent study of the  $\text{S-N}_2$  system at high pressures, which led to the characterisation of metastable  $\text{SN}_2$  (section 4.1).<sup>40</sup>

The main focus of early theoretical investigations of  $\text{SN}_4$  was an estimate of the aromaticity of the cyclic isomer, which is a  $6\pi$ -electron five-membered ring formally related to thiophene by the replacement of four CH units by four nitrogen atoms. Schleyer and co-workers calculated NICS (nucleus independent chemical shift) and NICS(1) values of  $-18.40$  and  $-17.48$  for *cyclo-SN*<sub>4</sub>; the large negative values are indicative of substantial aromatic character in the ring.<sup>42a</sup> This conclusion is supported by the calculated value of 18.56 for the ASE (aromatic stabilisation energy).<sup>42b</sup>

Nitrogen-rich sulfur nitrides are of considerable interest as high energy-density materials. The energy content of *cyclo-SN*<sub>4</sub> was first computed by Wang and co-workers using DFT methods at the B3LYP/6-311+G\*\* level.<sup>43</sup> It was found that *cyclo-SN*<sub>4</sub> is *ca.* 100 kcal mol<sup>-1</sup> higher in energy than the

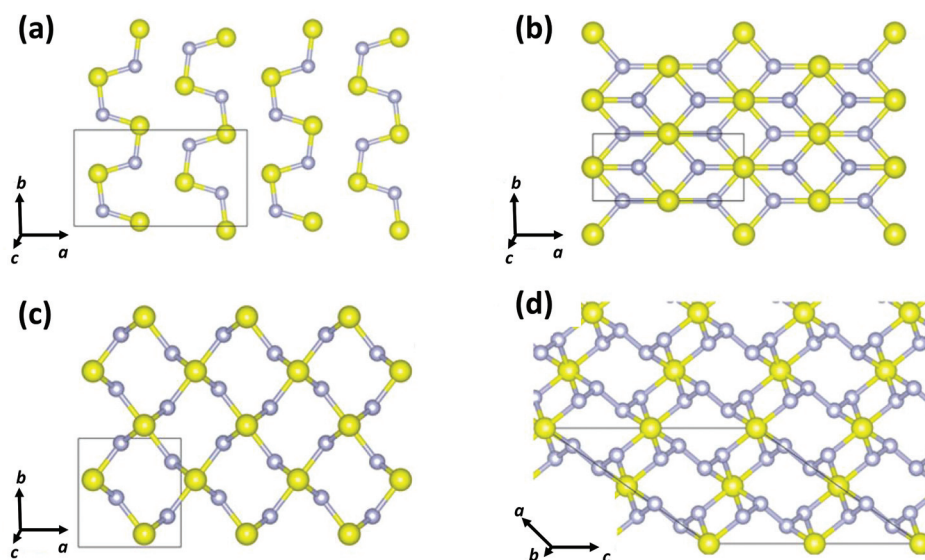
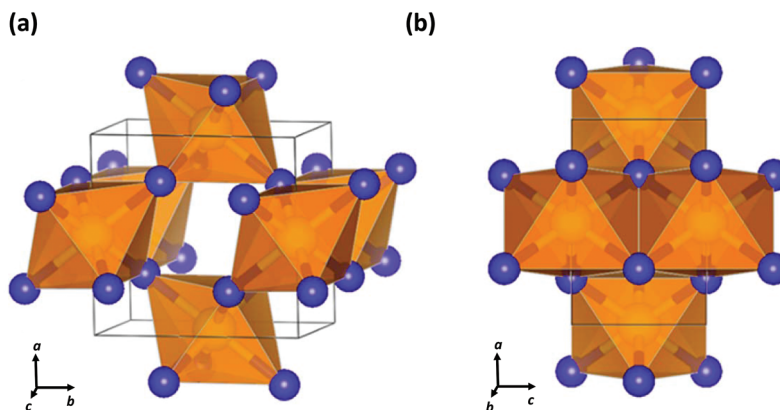


Fig. 7 Crystal structures of (a)  $Pnma$  ( $\text{SN}$ )<sub>x</sub>, (b)  $Immm$  ( $\text{SN}$ )<sub>x</sub>, (c)  $Pnnm$   $\text{SN}_2$ , and (d)  $C2/c$   $\text{SN}_4$ .<sup>39</sup> (Reproduced with permission from D. Li, F. Tian, Y. Z. Lv, S. Wei, D. Duan, B. Liu and T. Cui, *J. Phys. Chem. C*, 2017, **121**, 1515–1520. © 2017 The American Chemical Society.)





**Fig. 8** Crystal structure of  $\text{SN}_2$  formed at 81.6 GPa showing (a) the cross-linked octahedra and (b) the edge-sharing octahedra and apical S–N bonds.<sup>40</sup> (Reproduced with permission from D. Laniel, M. Bykov, T. Fedotenko, A. V. Ponomareva, I. A. Abrikosov, K. Glazyrin, V. Svitlyk, L. Dubrovinsky and N. Dubrovinskaia, *Inorg. Chem.*, 2019, **58**, 9195–9204. © 2019 The American Chemical Society.)

decomposition products  $1/8\text{S}_8 + \text{N}_2$ . However, the low dissociation barrier of  $7.0 \text{ kcal mol}^{-1}$  for the decomposition of  $\text{SN}_4$  into  $\text{N}_2 + \text{N}_2\text{S}$  (Scheme 4) precludes the isolation of this sulfur nitride under ambient conditions.<sup>44</sup>

#### 4.3. Dithiatetrazine $\text{S}_2\text{N}_4$

A planar six-membered ring *cyclo*- $\text{S}_2\text{N}_4$  would be an  $8\pi$ -electron (antiaromatic) system isoelectronic with dithiatriazines (RC)  $\text{S}_2\text{N}_3$ . The parent dithiatriazine ( $\text{R} = \text{H}$ ) is not known, but aryl derivatives ( $\text{R} = \text{Ph}$ ) exist as cofacial dimers in the solid state.<sup>1a</sup> Numerous acyclic and cyclic isomers are possible for the putative nitrogen-rich sulfur nitride  $\text{S}_2\text{N}_4$ . Schleyer and co-workers have carried out computational investigations of the thermochemical stability and kinetic persistence of various  $\text{S}_2\text{N}_4$  isomers at the B3LYP/6-311+G(3df) DFT level.<sup>13</sup> The results were compared with the corresponding data for the known sulfur nitrides  $\text{S}_2\text{N}_2$ ,  $\text{S}_4\text{N}_2$  and  $\text{S}_4\text{N}_4$ , as well as the nitrogen-rich species  $\text{SN}_4$  and  $\text{S}_3\text{N}_4$ . A boat conformation of 1,4- $\text{S}_2\text{N}_4$  (11), cf. 1,4- $\text{S}_2(\text{CH})_4$ , was predicted to be the most stable of the three possible six-membered rings. The other most thermodynamically stable isomers include two five-membered rings  $\text{SN}_4(=\text{S})$  (12 and 13) and two acyclic species  $\text{SNSNN}$  (14 and 15) (Scheme 5). From a consideration of the kinetic stability (dissociation barriers) of these five isomers it was concluded that the acyclic isomer 14 is the most viable candidate for synthesis. However, its dissociation barrier to give  $\text{N}_2$  and *cyclo*- $\text{S}_2\text{N}_2$  is only  $21.6 \text{ kcal mol}^{-1}$ , cf.  $51 \text{ kcal mol}^{-1}$  for *cyclo*- $\text{S}_2\text{N}_2$  (2,

$\text{E} = \text{S}$ ). Although this barrier is considerably higher than the value of  $7 \text{ kcal mol}^{-1}$  determined for the decomposition of *cyclo*- $\text{SN}_4$  (section 4.2), the facile formation of  $\text{S}_2\text{N}_2$  from decomposition of  $\text{SNSNN}$  (14) may account for the rapid production of  $(\text{SN})_x$  observed in the reaction of  $[\text{SNS}][\text{AsF}_6]$  with  $\text{CsN}_3$  in  $\text{SO}_2(\text{l})$  at  $-20^\circ\text{C}$ .<sup>45</sup>

As a general conclusion, it is important to note that kinetic stability is more important than thermodynamic stability in determining which binary sulfur–nitrogen species can be isolated under ambient conditions. The isomers of the nitrogen-rich cation  $[\text{S}_2\text{N}_3]^+$  a  $6\pi$ -electron system, provide a compelling example of this principle. Despite being less thermodynamically stable than the 1,3-isomer, the 1,2-isomer has been isolated and structurally characterised in the salt  $[\text{S}_2\text{N}_3]_2[\text{Hg}_2\text{Cl}_6]$ .<sup>46</sup> Although it is the only known *monocyclic*, nitrogen-rich S,N cation, several salts of the *tricyclic* cation  $[\text{S}_4\text{N}_5]^+$  have been structurally characterised.<sup>47</sup> The relative stability of 1,2- $[\text{S}_2\text{N}_3]^+$  is attributed to the higher dissociation barriers for its fragmentation compared to the 1,3-isomer for which the dissociation pathway to form  $[\text{SNS}]^+ + \text{N}_2$  has a barrier of only  $2.6 \text{ kcal mol}^{-1}$ .<sup>44a</sup>

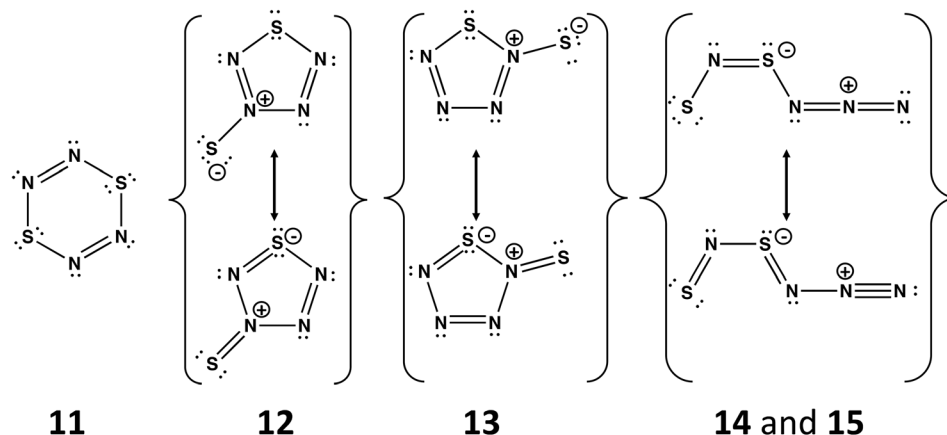
#### 4.4. Trithiatetrazepine $\text{S}_3\text{N}_4$

Planar, cyclic  $\text{S}_3\text{N}_4$  (16) would be a  $10\pi$ -electron (aromatic) system (see Scheme 6)<sup>48</sup> isoelectronic with the known trithiatetrazepine (HC) $\text{S}_3\text{N}_3$ .<sup>49</sup> However, the isolation of 16 at room temperature is unlikely in view the low energy barrier



**Scheme 4** The most facile dissociation pathway for *cyclo*- $\text{SN}_4$ .<sup>44</sup>





**Scheme 5** Structures of the five most stable isomers of  $S_2N_4$ . The acyclic isomers **14** and **15** differ only in the conformation; the  $-NNN$  fragment in **14** is oriented above the  $SNSN$ - plane, whereas **15** is planar.<sup>13</sup>



**Scheme 6**  $S_3N_4$  (**16**) and  $S_3N_3-NPPh_3$  (**17**).

(14.14 kcal mol<sup>-1</sup>) for dissociation into  $SNN$  and  $S_2N_2$ .<sup>13</sup> The known compound  $S_3N_3-N=PPh_3$  (**17**) formed from the reaction of  $S_4N_4$  with  $PPh_3$  *via* ring contraction can be considered as the triphenylphosphine adduct of  $S_3N_4$ .<sup>50</sup> It is also noted that the related derivative  $S_3N_3-N=S$  has been identified as a short-lived intermediate generated upon flash photolysis of  $S_4N_4$ .<sup>51</sup>

## 5. Nitrogen-rich selenium nitrides

As mentioned in section 1, the only binary selenium nitride that has been isolated under ambient conditions and structurally characterised is  $Se_4N_4$  (**1**,  $E = Se$ ),<sup>3a</sup> although metal complexes of  $Se_2N_2$  (**2**,  $E = Se$ ) are also known.<sup>3c,d</sup> In that context investigations of the high-pressure phase diagrams of the binary selenium–nitrogen system by Cui and co-workers reported in 2019 are of considerable interest.<sup>52</sup> These authors identified four stable compounds at high pressures:  $Cmc2_1-SeN_2$ ,  $P2_1/m-SeN_3$ ,  $P\bar{1}-SeN_4$  and  $P\bar{1}-SeN_5$ . As illustrated in Fig. 9, these novel nitrogen-rich materials are predicted to incorporate a variety of polynitrogen arrangements in the solid state.<sup>52</sup>

The binary selenium nitride  $Cmc2_1-SeN_2$  has a layer structure (Fig. 9a), while  $P2_1/m-SeN_3$ ,  $P\bar{1}-SeN_4$  and  $P\bar{1}-SeN_5$  incorporate  $N_\infty$ -chains (Fig. 9b), oligomeric  $N_8$ -chains (Fig. 9c) or distorted  $[N_6]^{3-}$  anionic rings alternating with layers of  $N_\infty$ -chains (Fig. 9d). The high energy-content of the latter three phases is

reflected in the values of their energy densities, which are 3.27, 3.26 and 4.08 kJ g<sup>-1</sup>, respectively.<sup>52</sup>

Information on the dissociation barriers for these binary selenium nitrides is not available.

## 6. Ternary S,N,P molecules

A phosphorus atom P has the same number of electrons as an  $S^+$  cation, consequently there can be an isoelectronic relationship between certain ternary S,N,P neutral molecules and well-known binary S,N cations. The latter species can be isolated as thermally stable salts, which have been structurally characterised, and the cations have been shown to exhibit a range of chemical reactions.<sup>1a,b</sup> The recent identification of the ternary systems  $SNP$ <sup>12a</sup> and  $SP_2N_2$ <sup>12b</sup> provide cogent examples of this isoelectronic connection.

Francisco, Zeng *et al.*, conducted an initial investigation of the pyrolysis and photolysis of the triazide  $SP(N_3)_3$ .<sup>12a</sup> The experimental work was presaged by DFT calculations of the three triatomic SNP isomers, *viz.* linear SNP (**18**), linear SPN (**19**) and the three-membered ring *cyclo*-PSN (thiazaphosphirine) (**20**) at the B3LYP/6-311+G(3df). As indicated in Fig. 10, the cyclic isomer **20** is separated from the linear isomers **18** and **19** by barriers of 138 and 95 kJ mol<sup>-1</sup>, respectively; the SNP arrangement **18** was predicted to be the global minimum. In one experimental approach the pyrolysis of  $SP(N_3)_3$  at



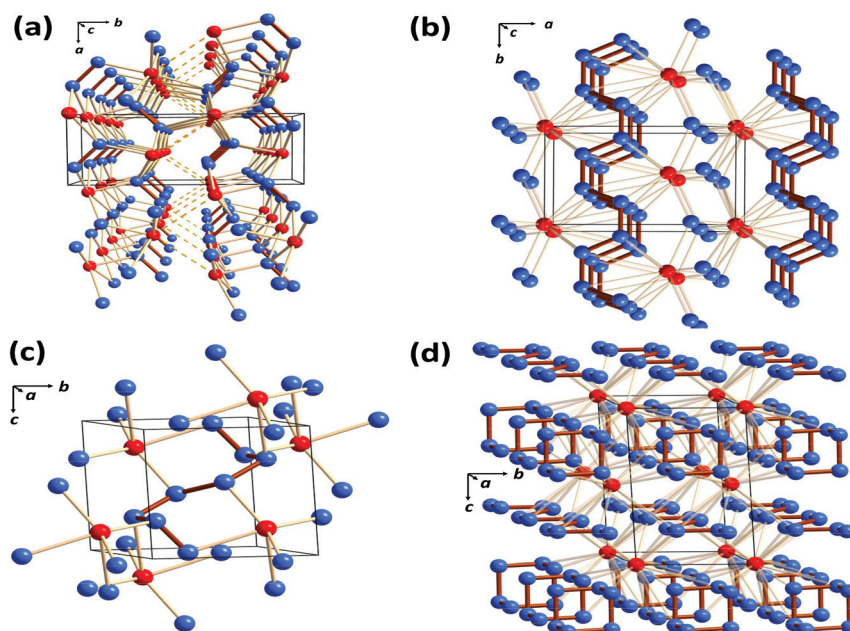


Fig. 9 Crystal structures of the predicted selenium nitrides: (a)  $Cmc2_1$ - $SeN_2$  at 90 GPa (b)  $P2_1/m$ - $SeN_3$  at 80 GPa (c)  $P1$ - $SeN_4$  at 140 GPa and (d)  $P1$ - $SeN_5$  at 130 GPa. Selenium atoms are depicted in red and nitrogen atoms in blue (redrawn from the structural data in ref. 52).



Fig. 10 Calculated reaction coordinate of SPN isomers 18–20; bond lengths are given in Å.<sup>12a</sup> (Reproduced with permission from X. Zeng, H. Beckers, H. Willner and J. S. Francisco, *Angew. Chem., Int. Ed.*, 2012, 51, 3334–3339. © 2012 WILEY-VCH Verlag GmbH & Co. KGaA, Weinheim.)

1000 °C followed by trapping of the products in an argon matrix at 16 K generated SPN (19) [eqn (1)]. This species was identified with the help of  $^{15}N$ -labelling by comparison of calculated and experimental IR frequencies, which also revealed the formation of other nitrogen-containing species, PN, SN and  $SN_2$ .<sup>12a</sup>



In an alternative procedure the photolysis of  $SP(N_3)_3$  in solid argon resulted in a stepwise dissociation to give the most stable SNP isomer 18 as the final product. In both the pyrolysis and photolysis experiments selective UV irradiation produced

the linear SPN (19) and *cyclo*-PSN (20), which were identified by IR spectroscopy.<sup>12a</sup>

The structure of SNP (18) can be represented by the two Lewis structures shown in Fig. 11a. The calculated P–N bond length is 1.502 Å, slightly greater than the sum of the triple bond radii for P and N (1.48 Å), and the calculated P–N stretching frequency of 1314  $cm^{-1}$  is close to that of diatomic PN (1327  $cm^{-1}$ ).<sup>12a</sup> The SNP isomer (18) is isoelectronic with the

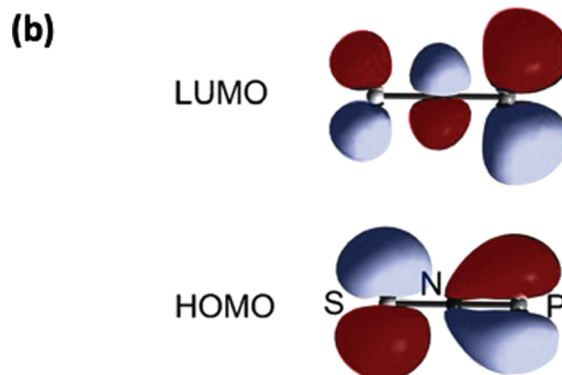


Fig. 11 (a) Lewis resonance structures and (b) HOMO and LUMO of the isomer SNP.<sup>12</sup> (Reproduced with permission from X. Zeng, H. Beckers, H. Willner and J. S. Francisco, *Angew. Chem., Int. Ed.*, 2012, 51, 3334–3339. © 2012 WILEY-VCH Verlag GmbH & Co. KGaA, Weinheim.)



linear sulfur–nitrogen cation  $[\text{SNS}]^+$ , which has an extensive cycloaddition chemistry.<sup>53</sup> The similarity of the frontier orbitals of SNP (18) (Fig. 11b) with those of  $[\text{SNS}]^+$  suggest that the ephemeral SNP species could be trapped *via* cycloaddition reactions, e.g. with alkynes or nitriles.

A subsequent IR analysis of the products of the flash pyrolysis of  $\text{SP}(\text{N}_3)_3$  under conditions used to generate SNP (18) (*vide supra*) revealed a new species with IR frequencies that increased in intensity with prolonged deposition time.<sup>12b</sup> The mid- and far-IR frequencies of this product appeared as quartets when  $^{15}\text{N}$  labelled  $\text{SP}(\text{N}_3)_3$  was used as a precursor, indicating a molecule with two structurally non-equivalent N atoms.<sup>12b</sup> In order to elucidate the identity of this species, theoretical calculations of the dimerisation of SNP were carried out. As illustrated in Fig. 12, the activation energy for head-to-tail association of SNP to give *cyclo*-SNPSNP is low. However, the structural equivalence of the two nitrogen atoms in this six-membered ring rules it out as the source of the new IR bands. Instead, the energetically favourable loss of a sulfur atom from *cyclo*-SNPSNP, which is formally an  $8\pi$ -electron system, to give the five-membered ring *cyclo*-SNPNP (2,4-diphospha-3,5-diaza-thiole), a  $6\pi$ -electron system, is invoked to explain the observed and calculated IR data (Fig. 12).<sup>12b</sup>

The aromatic nature of *cyclo*-SNPNP, which is isoelectronic with the known sulfur–nitrogen dication  $[\text{S}_3\text{N}_2]^{2+}$ ,<sup>1a</sup> may con-

tribute to its stability. However, the  $6\pi$ -electron cation *cyclo*- $[\text{SNSNP}]^+$  is expected to exhibit higher stability owing to the positive charge and possible isolation as a salt. By analogy with the cycloaddition of  $[\text{NS}]^+$  with  $[\text{SNS}]^+$  to give  $[\text{S}_3\text{N}_2]^{2+}$ ,<sup>53</sup> cycloaddition of SNP with an  $[\text{NS}]^+$  salt could generate the putative cation *cyclo*- $[\text{SNSNP}]^+$ .

A third example of the isoelectronic relationship between ternary S,N,P molecules and binary S,N cations involves the well-known planar, cyclic cation  $[\text{S}_4\text{N}_4]^{2+}$ , a fully delocalised  $10\pi$ -electron system.<sup>1a</sup> The replacement of two antipodal S atoms in the supposed planar molecule  $\text{S}_4\text{N}_4$  by P atoms generates 1,5- $\text{P}_2\text{N}_4\text{S}_2$ , isoelectronic with  $[\text{S}_4\text{N}_4]^{2+}$ . According to Gleiter, this ternary S,N,P molecule would incorporate an unpaired 3p electron at each P centre (21).<sup>7a</sup> The diradical species 21 would be stabilised by addition of two radicals  $\text{R}^\cdot$  at the phosphorus centres to give  $\text{RP}(\text{NSN})_2\text{PR}$  (22) with two  $4\pi$ -electron  $-\text{N}=\text{S}=\text{N}-$  groups bridging the two  $\text{RP}^{\text{III}}$  centres (Scheme 7). Although the free ligand is not known, metal complexes of 22 ( $\text{R} = ^t\text{Bu}$ ,  $\text{N}^i\text{Pr}_2$ ) in which the  $\text{P}_2\text{N}_4\text{S}_2$  ring is almost planar have been structurally characterized 30 years ago.<sup>54</sup>

The aromatic character of 1,5- $\text{P}_2\text{N}_4\text{S}_2$  (21) has been compared with that of the isoelectronic  $10\pi$ -electron heterocycle dithiatetrazocine  $(\text{HC})_2\text{N}_4\text{S}_2$  using density functional methods.<sup>55,56</sup> It was found that replacement of the two HC groups by the more electronegative P atoms decreases the aromatic character.<sup>55</sup> However, the ternary ring system was suggested to be a reasonable synthetic target.

In contrast to the planar P(III)-containing heterocycle 22, the corresponding P(V) systems  $\text{R}_2\text{P}(\text{NSN})_2\text{PR}_2$  (1,5-diphosphadithiatetrazocines) form bicyclic structures with a weak transannular S...S interaction similar to that discussed for  $\text{S}_4\text{N}_4$  in section 3.1.1. A recent fragment-based energy analysis by Jacobsen estimates that the cross-ring connection in 1,5-diphosphadithiatetrazocines is about half as strong as a typical S–S bond.<sup>57</sup> This class of S,N,P heterocycle is considered to be an unusual inorganic example of bishomoaromaticity.<sup>7a,58</sup>

## 7. Summary and outlook

Although the complexities of the electronic structures of the well-known binary sulfur nitrides  $\text{S}_2\text{N}_2$  and  $\text{S}_4\text{N}_4$  and their selenium analogues are still under consideration, the focus of recent investigations of this class of inorganic compounds has been on the potential applications of both known and

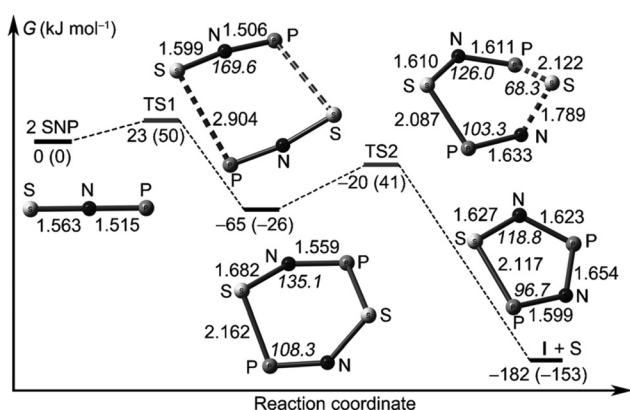
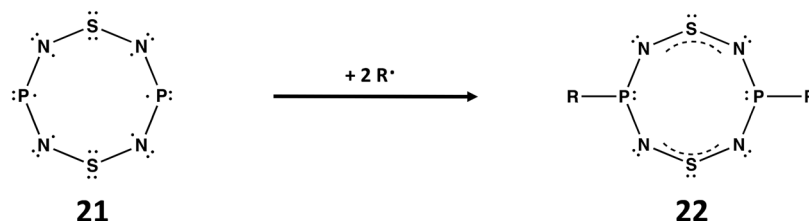


Fig. 12 Head-to-tail dimerisation of SNP and subsequent formation of *cyclo*-SNPNP; relative energies ( $\text{kJ mol}^{-1}$ ) and computed bond lengths ( $\text{\AA}$ ) at the B3LYP/6-311+G(3df) level.<sup>13</sup> (Reproduced with permission from X. Zeng, H. Li, H. Sun, H. Beckers, H. Willner and H. F. Schaefer III, *Angew. Chem., Int. Ed.*, 2015, 54, 1327–1330. © 2015 WILEY-VCH Verlag GmbH & Co. KGaA, Weinheim.)



Scheme 7 Stabilisation of  $\text{P}_2\text{N}_4\text{S}_2$  (21) by reaction with two  $\text{R}^\cdot$  radicals to give  $\text{RP}(\text{NSN})_2\text{PR}$  (22).<sup>7a</sup>



unknown systems. The foremost example is the use of the facile transformation of  $S_2N_2$  into the blue-black polymer  $(SN)_x$  for the detection of fingerprints on metal surfaces, which is being considered as an alternative to existing processes for this application in forensic science (section 3.2.4). A more speculative function involves the possible use of  $S_2N_2$  or other sulfur–nitrogen rings as hydrogen-storage materials (section 3.2.5). Although the feasibility of this application is questionable in the case of  $S_2N_2$ , sulfur–nitrogen systems with higher chemical and thermal stability, e.g. C,S,N heterocycles, may be worthy of computational and experimental interrogation for this purpose.

In the area of sulfur-rich nitrides, the unknown molecule  $S_3N_2$  is predicted to have quite different properties compared to those of the well-characterised six-membered ring 1,3- $S_4N_2$ , which is a labile, low melting compound. By contrast, computational studies indicate that crystalline  $S_3N_2$  will form a two-dimensional network involving only  $\sigma$  bonds rather than an  $8\pi$ -electron five-membered ring. Furthermore, it has been proposed that  $S_3N_2$  will exhibit chemical and thermal stability and behave as a wide direct band gap semiconductor with possible optoelectronic applications. As suggested in section 2, this neutral sulfur nitride should be experimentally accessible under ambient conditions so that these predictions can be tested.

Nitrogen-rich sulfur nitrides, e.g. thiatetrazole *cyclo*- $SN_4$ , have long been considered as potential high energy-density materials (section 4.2). Until recently, this purported 5-membered ring and the acyclic triatomic molecule NSN have only been invoked as fleeting intermediates in the decomposition of sulfur–nitrogen ring systems. In the last few years, however, seminal experimental and computational studies of the combination of a chalcogen (sulfur or selenium) and nitrogen gas ( $N_2$ ) at very high pressures have yielded unanticipated information about the structures and properties of this new class of chalcogen nitride. In general, the computational work indicates that at high pressures a variety of nitrogen-rich compounds with structures that are quite different from the metastable sulfur nitrides known to exist at ambient temperatures and pressures (Scheme 1) will be formed. Experimental verification of this prediction has been provided by the identification of an  $SN_2$  solid at pressures above 64 GPa. This novel material has a  $CaCl_2$  structure comprised of  $SN_6$  octahedra with triply coordinated N atoms, as forecasted by earlier computational work (section 4.1). In the light of these experimental results, the predicted formation of stable binary selenium nitrides  $SeN_x$  ( $x = 2, 3, 4$  or 5) at high pressures should provide an incentive for an experimental study of the selenium– $N_2$  system with the characterisation of the elusive  $(SeN)_x$  polymer as one of the target molecules.

Finally, recently characterised acyclic and cyclic neutral S,N,P molecules are considered in the context of the known structures and reactions of binary sulfur–nitrogen cations, which are isoelectronic with the ternary S,N,P systems. This comparison is intended to provide some guidance to the future development of the chemistry of these interesting ternary systems.

## Conflicts of interest

There are no conflicts of interest to declare.

## Acknowledgements

The authors thank an anonymous reviewer for the suggestion of computational and experimental investigations of the reaction  $S_4N_4$  with molecular  $H_2$ , which they had been considering. They are also grateful to Professor Dennis Salahub (University of Calgary) for helpful discussions of the electronic structure of  $S_4N_4$ .

## References

- (a) T. Chivers, *A Guide to Chalcogen-Nitrogen Chemistry*, World Scientific Publishing Co., Singapore, 2005; (b) T. Chivers and R. S. Laitinen, in *Handbook of Chalcogen-Nitrogen Chemistry: New Perspectives in Sulfur, Selenium and Tellurium*, ed. F. A. Devillanova and W.-W. du Mont, 2nd edn, 2013, ch. 4, vol. 1; (c) The chemistry of the ephemeral monomeric radical species NE (E = S, Se, Te) is covered comprehensively in a recent book chapter. R. T. Boeré and T. Roemmele, in *Comprehensive Inorganic Chemistry II*, ed. J. Reedijk and K. Poeppelmeier, Elsevier, Oxford, 2013, ch. 1.14, vol. 1, pp. 375–411.
- (a)  $S_4N_4$ : M. L. Delucia and P. Coppens, *Inorg. Chem.*, 1978, **17**, 2336–2338; (b)  $S_2N_2$ : C. M. Mikulski, P. J. Russo, M. S. Soran, A. G. MacDiarmid, A. F. Garito and A. J. Heeger, *J. Am. Chem. Soc.*, 1975, **97**, 6358–6363; (c)  $(SN)_x$ : M. J. Cohen, A. F. Garito, A. J. Heeger, A. G. MacDiarmid, C. M. Mikulski, M. S. Soran and J. Kleppinger, *J. Am. Chem. Soc.*, 1976, **98**, 3844–3848; (d)  $S_4N_2$ : T. Chivers, P. W. Coddling, W. G. Laidlaw, S. W. Liblong, R. T. Oakley and M. Trsic, *J. Am. Chem. Soc.*, 1983, **105**, 1186–1192; (e)  $S_5N_6$ : T. Chivers and J. Proctor, *J. Chem. Soc., Chem. Commun.*, 1978, 642–643.
- (a)  $Se_4N_4$ : H. Folkerts, B. Neumüller and K. Dehnicke, *Z. Anorg. Allg. Chem.*, 1994, **620**, 1011–1015, and references cited therein; (b)  $Se_2S_2N_4$ : A. Maaninen, J. Siivari, R. S. Laitinen and T. Chivers, *Inorg. Chem.*, 1999, **38**, 3450–3454; (c)  $Se_2N_2$ : P. F. Kelly and A. M. Z. Slawin, *J. Chem. Soc., Dalton Trans.*, 1996, 4029–4030; (d) P. F. Kelly and A. M. Z. Slawin, *Angew. Chem., Int. Ed. Engl.*, 1995, **34**, 1758–1759.
- The black powder obtained from the reaction of  $Se_2Cl_2$  with trimethylsilyl azide in dichloromethane was originally claimed to be  $Se_4N_2$ , but it was subsequently identified as the selenium–nitrogen chloride  $Se_3N_2Cl_2$ . (a) K. Dehnicke, F. Schmock, K. F. Kohler and G. Frenking, *Angew. Chem., Int. Ed. Engl.*, 1991, **30**, 577; (b) T. Chivers, J. Siivari and R. S. Laitinen, *Angew. Chem., Int. Ed. Engl.*, 1992, **31**, 1518–1519.



- 5 A. Maaninen, J. Siivari, R. S. Laitinen and T. Chivers, *Inorg. Chem.*, 1997, **36**, 2170–2177.
- 6 For a summary of the literature prior to 2012, see: J. Moilanen, A. J. Karttunen, H. M. Tuononen and T. Chivers, *J. Chem. Theory Comput.*, 2012, **8**, 4249–4258.
- 7 (a) R. Gleiter, G. Haberhauer and S. Woitschetzki, *Chem. – Eur. J.*, 2014, **20**, 13801–13810; (b) R. Gleiter and G. Haberhauer, *Coord. Chem. Rev.*, 2017, **344**, 263–298.
- 8 T. T. Takaluoma, K. Laasonen and R. S. Laitinen, *Inorg. Chem.*, 2013, **52**, 4648–4657.
- 9 (a) R. S. P. King, P. F. Kelly, S. E. Dean and R. J. Mortimer, *Chem. Commun.*, 2007, 4812–4814; (b) P. F. Kelly, R. S. P. King and R. J. Mortimer, *Chem. Commun.*, 2008, 6111–6113; (c) S. M. Bleay, P. F. Kelly and R. S. B. King, *J. Mater. Chem.*, 2010, **20**, 10100–10102; (d) S. M. Bleay, P. F. Kelly, R. S. P. King and S. G. Thorngate, *Sci. Justice*, 2019, **59**, 606–621. The identity of the S<sub>2</sub>N<sub>2</sub> precursor is not revealed in this paper.
- 10 (a) H. Xiao, X. Shi, X. Liao, Y. Zhang and X. Chen, *Phys. Rev. Mater.*, 2018, **2**, 024002; (b) Y. Chen, X. Liao, X. Shi, H. Xiao, Y. Liu and X. Chen, *Phys. Chem. Chem. Phys.*, 2019, **21**, 5916–5924; (c) Auxetic materials become thicker when stretched and thinner in response to compression.
- 11 For a recent review of the fundamental chemistry of binary S<sub>2</sub>N and ternary S<sub>2</sub>N<sub>2</sub>O anions, see: T. Chivers and R. S. Laitinen, *Chem. Soc. Rev.*, 2017, **46**, 5182–5192.
- 12 (a) X. Zeng, H. Beckers, H. Willner and J. S. Francisco, *Angew. Chem., Int. Ed.*, 2012, **51**, 3334–3339; (b) X. Zeng, H. Li, H. Sun, H. Beckers, H. Willner and H. F. Schaefer III, *Angew. Chem., Int. Ed.*, 2015, **54**, 1327–1330.
- 13 G.-H. Zhang, Y.-F. Zhao, J. I. Wu and P. V. R. Schleyer, *Inorg. Chem.*, 2012, **51**, 13321.
- 14 T. Chivers and R. S. Laitinen, *Dalton Trans.*, 2017, **46**, 1357–1367.
- 15 (a) J. Contreras-Garcia, E. R. Johnson, S. Keinan, R. Chaudret, J.-P. Piquemal, D. N. Beratan and W. Yang, *J. Chem. Theory Comput.*, 2011, **7**, 625–632; (b) the energies of strong hydrogen bonds falls within the range 15–40 kcal mol<sup>−1</sup>.
- 16 R. Mews, *J. Fluorine Chem.*, 1981, **18**, 155–158.
- 17 Y. Xu, T. Xu, D. Jiajun, S. R. Kirk and S. Jenkins, *Int. J. Quantum Chem.*, 2016, **116**, 1025–1039.
- 18 J. Konu, T. Bajorek, R. S. Laitinen, T. Chivers, R. J. Suontamo and M. Ahlgrén, *Eur. J. Inorg. Chem.*, 2006, 2951–2958, and references cited therein.
- 19 M. K. Si and B. Ganguly, *Chem. Phys. Lett.*, 2018, **713**, 160–165.
- 20 D. V. Konarev, E. F. Valeev, Y. L. Slovokhotov and R. N. Lyobovskaya, *J. Phys. Chem. Solids*, 1997, **58**, 1865–1867.
- 21 A. Maaninen, J. Siivari, R. S. Laitinen and T. Chivers, *Inorg. Synth.*, 2002, **33**, 196–199.
- 22 A. Ghosh and S. Berg, *Arrow Pushing in Inorganic Chemistry: A Logical Approach to the Chemistry of the Main-Group Elements*, John Wiley & Sons, Inc., New Jersey, 2014, pp. 240–243.
- 23 (a) B. G. Kumar and K. Muralidharan, *Eur. J. Inorg. Chem.*, 2013, 2102–2108; (b) B. G. Kumar and K. Muralidharan, *J. Mater. Chem.*, 2011, **21**, 11271–11275; (c) B. G. Kumar and K. Muralidharan, *RSC Adv.*, 2014, **4**, 28219–28224; (d) Cyclic sulfur imides of the type (SNR)<sub>4</sub> (R = Me, Et, Bz) have been characterised as colourless crystalline solids, but the corresponding polymers (SNR)<sub>n</sub> are unknown. H. G. Heal, *The Inorganic Heterocyclic Chemistry of Sulfur, Nitrogen and Phosphorus*, Academic Press Inc., London, U.K., 1980, pp. 16–40.
- 24 T. L. Roemmele, J. Konu, R. T. Boéré and T. Chivers, *Inorg. Chem.*, 2009, **48**, 9454–9462.
- 25 For an authoritative summary of earlier theoretical calculations for S<sub>2</sub>N<sub>2</sub> see: P. B. Karadakov, M. A. H. Al-Yassiri and D. L. Cooper, *Chem. – Eur. J.*, 2018, **24**, 16791–16803.
- 26 Y. Jung, T. Heine, P. V. R. Schleyer and M. Head-Gordon, *J. Am. Chem. Soc.*, 2004, **126**, 3132–3138.
- 27 (a) H. M. Tuononen, R. Suontamo, J. Valkonen and R. S. Laitinen, *J. Phys. Chem. A*, 2004, **108**, 5670–5677; (b) H. M. Tuononen, R. Suontamo, J. Valkonen and R. S. Laitinen, *J. Phys. Chem. A*, 2005, **109**, 6309–6317.
- 28 B. Braida, A. Lo and P. C. Hiberty, *ChemPhysChem*, 2012, **13**, 811–819.
- 29 R. D. Harcourt, *ChemPhysChem*, 2013, **14**, 2859–2864.
- 30 R. Evans, A. J. Downs, R. Köppe and S. C. Peake, *J. Phys. Chem. A*, 2011, **115**, 5127–5137. The IR frequencies of S<sub>2</sub>N<sub>2</sub> in the solid, vapour and matrix-isolated states obtained in previous studies are summarized in Table 3 of this paper.
- 31 A. Perrin, A. F. Antognini, X. Zeng, H. Beckers, H. Willner and G. Rauhut, *Chem. – Eur. J.*, 2014, **20**, 10323–10331.
- 32 W. Zou, D. Izotov and D. Cremer, *J. Phys. Chem. A*, 2011, **115**, 8731–8742.
- 33 A. J. Bridgeman and B. Cunningham, *Spectrochim. Acta, Part A*, 2004, **60**, 471–480.
- 34 X. Zeng, A. F. Antognini, H. Beckers and H. Willner, *Angew. Chem., Int. Ed.*, 2015, **54**, 2758–2761.
- 35 A. Datta, *Phys. Chem. Chem. Phys.*, 2009, **11**, 11054–11059.
- 36 C. Wentrup and P. Kambouris, *Chem. Rev.*, 1991, **91**, 363–373.
- 37 J.-H. Lin, H. Zhang, X.-L. Cheng and Y. Miyamoto, *Phys. Rev. B*, 2016, **94**, 195404.
- 38 F. Li, X. Lv, J. Gu, K. Tu, J. Gong, P. Jin and Z. Chen, *Nanoscale*, 2020, **12**, 85–92.
- 39 D. Li, F. Tian, Y. Z. Lv, S. Wei, D. Duan, B. Liu and T. Cui, *J. Phys. Chem. C*, 2017, **121**, 1515–1520.
- 40 D. Laniel, M. Bykov, T. Fedotenko, A. V. Ponomareva, I. A. Abrikosov, K. Glazyrin, V. Svitlyk, L. Dubrovinsky and N. Dubrovinskaya, *Inorg. Chem.*, 2019, **58**, 9195–9204.
- 41 T. Klapötke and A. Schulz, *Polyhedron*, 1996, **15**, 4387–4390.
- 42 (a) M. K. Cyrański, T. M. Krygowski, A. R. Katritzky and P. V. R. Schleyer, *J. Org. Chem.*, 2002, **67**, 1333–1338; (b) M. K. Cyrański, P. V. R. Schleyer, T. M. Krygowski, H. Jiao and G. Hohlneicher, *Tetrahedron*, 2003, **59**, 1657–1665.
- 43 (a) L. J. Wang, P. G. Mezey and M. Z. Zgierski, *Chem. Phys. Lett.*, 2003, **369**, 386–393; (b) L. J. Wang and P. G. Mezey, *Chem. Phys. Lett.*, 2004, **387**, 233–237.
- 44 (a) G.-H. Zhang, Y.-F. Zhao, J. I. Wu and P. V. R. Schleyer, *Inorg. Chem.*, 2009, **48**, 6773–6780; (b) The molecular struc-



- ture, IR and UV spectra of  $\text{SN}_4$  have been calculated by a modification of DFT; a strong absorption at 212 nm is predicted. D. Glossman-Mitnik, *Theor. Chem. Acc.*, 2007, **117**, 57–68.
- 45 F. A. Kennett, G. K. MacLean, J. Passmore and M. N. S. Rao, *J. Chem. Soc., Dalton Trans.*, 1982, 851–857.
- 46 S. Herler, P. Mayer, H. Nöth, A. Schulz, M. Suter and M. Vogt, *Angew. Chem., Int. Ed.*, 2001, **40**, 3173–3175.
- 47 T. Chivers, L. Fielding, W. G. Laidlaw and M. Trsic, *Inorg. Chem.*, 1979, **18**, 3379–3388.
- 48 P. W. Fowler, C. W. Rees and A. Soncini, *J. Am. Chem. Soc.*, 2004, **126**, 11202–11212.
- 49 P. J. Dunn, J. L. Morris and C. W. Rees, *J. Chem. Soc., Perkin Trans. 1*, 1988, 1745–1748.
- 50 J. Bojes, T. Chivers, A. W. Cordes, G. MacLean and R. T. Oakley, *Inorg. Chem.*, 1981, **20**, 16–21, and references cited therein.
- 51 E. A. Pritchina, D. S. Terpilovskaya, Y. P. Tsentalovich, H. S. Platz and N. P. Gritsan, *Inorg. Chem.*, 2012, **51**, 4747–4755.
- 52 W. Wang, H. Wang, Y. Liu, F. Tian, D. Duan, H. Yu and T. Cui, *Inorg. Chem.*, 2019, **58**, 2397–2402.
- 53 S. Parsons and J. Passmore, *Acc. Chem. Res.*, 1994, **27**, 101–108, and references cited therein.
- 54 T. Chivers, K. S. Dhathathreyan, C. Lensink, A. Meetsma, J. C. van de Grampel and J. L. de Boer, *Inorg. Chem.*, 1989, **28**, 4150–4154.
- 55 A. G. Papadopoulos, N. D. Charistos and A. Muñoz-Castro, *New J. Chem.*, 2016, **40**, 5090–5098.
- 56 K. H. Moock, K. M. Wong and R. T. Boéré, *Dalton Trans.*, 2011, **40**, 11599–11604.
- 57 H. Jacobsen, *Inorg. Chem.*, 2013, **52**, 11843–11849.
- 58 For a discussion of the nature of the transannular  $\text{S}\cdots\text{S}$  interaction in 1,5-diphosphadithiatetrazocines, including the concept of bishomoaromaticity, see: (a) Q. Zhang, S. Yue, X. Lu, Z. Chen, R. Huang, L. Zheng and P. V. R. Schleyer, *J. Am. Chem. Soc.*, 2009, **131**, 9789–9799; (b) H. S. Rzepa, *Nat. Chem.*, 2009, **1**, 510–512; (c) T. Chivers, R. W. Hilts, P. Jin, Z. Chen and X. Lu, *Inorg. Chem.*, 2010, **49**, 3810–3816.

